Laser Physics, Vol. 10, No. 2, 2000, pp. 495–500.

Applications of Femtosecond Lasers in Corneal Surgery

T. Juhasz*, **, G. Djotyan*, **, F. H. Loesel*, ***, R. M. Kurtz*, **, C. Horvath*, ***, J. F. Bille***, and G. Mourou***

** Center for Ultrafast Optical Science, University of Michigan, 1006 IST Building, 2200 Bonisteel Blvd., Ann Arbor, MI 48109-2099, USA*

*** Kellogg Eye Center, Department of Ophthalmology, University of Michigan, 1000 Wall Street, Ann Arbor, MI 48105, USA*

**** Institute for Applied Physics, University of Heidelberg, Albert-Ueberle-Str. 3-5, D-69120 Heidelberg, Germany*

***** Research Institute for Particle & Nuclear Physics, XII. Konkoly Thege ut. 29-33, H-1525, Budapest, P.O. Box 49, Hungary*

e-mail: djotjan@rmki.kfki.hu

Received July 21, 1999

Abstract—We investigated potential applications of ultrashort (femtosecond) pulsed laser technology in corneal refractive surgery. When compared with longer pulsewidth nanosecond or picosecond laser radiation, femtosecond laser-tissue interactions are characterized by significantly smaller and more deterministic photodisruptive energy thresholds, as well as reduced shock waves and smaller cavitation bubbles. Femtosecond laser technology may be able to perform a variety of corneal refractive procedures with high precision, offering advantages over current mechanical and laser devices and techniques, enabling entirely new approaches for refractive surgery. An analytically solvable shell model has been developed to predict the results of completely intrastromal incisionless surgery for myopic and hyperopic refractive corrections.

I. INTRODUCTION

Ultrashort laser radiation has attracted significant interest in surgical applications, particularly for corneal refractive surgery. This surgical correction of myopia (short-sightedness), hyperopia (far-sightedness) and astigmatism has become the most commonly performed clinical laser procedure. In this surgery, the curvature of the cornea is altered by removing a specific amount of corneal tissue with ultraviolet photoablation from the excimer laser. Two excimer techniques are now in widespread use, photorefractive keratectomy (PRK) and laser-assisted in situ keratomileusis (LASIK). LASIK now dominates the field due to its minimal effect on the corneal surface, which reduces pain and recovery time. However, LASIK requires the use of a mechanical blade (microkeratome) to give the excimer laser access to deeper corneal layers.

In contrast to eximer lasers, the near-infrared (near-IR) radiation of photodisruptive lasers is not absorbed (at least to the first order) by the ocular media [1, 2]. Near-IR pulses can pass through transparent and limited thickness translucent material, affecting tissue only at the focus of the laser beam (e.g., [2–5]). Photodisruption takes place via laser induced optical breakdown (LIOB), which requires focusing to a small focal spot size to achieve a threshold fluence for plasma formation (e.g., [6–9]). The generated micro-plasma absorbs more laser energy than the surrounding tissue, leading to supersonic expansion of the plasma. This expansion is accompanied by secondary effects, such as shock wave emission, cavitation and gas bubble generation [10–13], resulting in disruption of the tissue within the focal volume of the laser.

Since the energy fluence threshold for LIOB decreases with decreasing pulse duration, one can use low energy laser pulses, thereby reducing the shock wave range and the cavitation bubble size (see [4, 8, 9, 14–19]). Under these conditions, damage to non-targeted tissue is diminished and the precision and predictability of the surgery is increased.

We evaluated the potential use of femtosecond lasers for performing minimally-invasive and highly-localized corneal surgical procedures, identifying practically no collateral tissue damage. The availability of practical femtosecond laser surgical tools may lead to significantly improved ophthalmic surgical procedures and techniques.

We developed an analytically solvable shell model of cornea to predict the results of such corneal refractive procedures in which the cornea is considered as a thin elastic spherical shell. This model allows us to take into account the inhomogeneities induced in the cornea by completely intrastromal femtosecond laser pulse techniques in which a portion of the treated tissue remains inside the stroma, although with altered structural characteristics.

II. INTERACTION OF FEMTOSECOND LASER PULSES WITH CORNEAL TISSUE

While it has been known for some time that decreasing pulse duration into the femtosecond time regime significantly reduces the threshold for optical breakdown (e.g., [4, 6, 8]), the specific characteristics of these effects have important practical implications. In Fig. 1, the threshold fluence of optical breakdown is

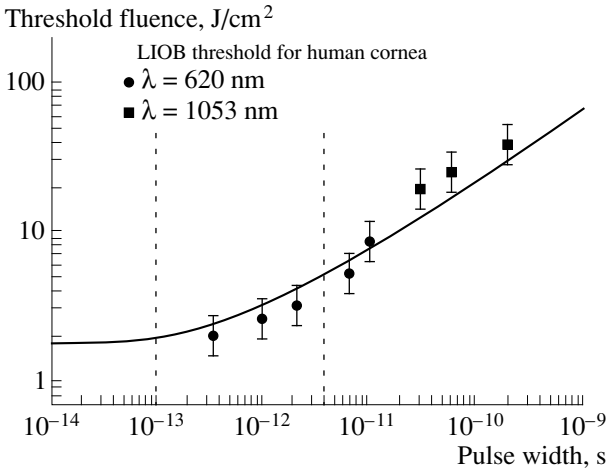

Fig. 1. Fluence at threshold for laser induced optical breakdown (LIOB) as a function of laser pulse width as measured on the surface of human cornea. Solid line shows model curve fitting (see [8]).

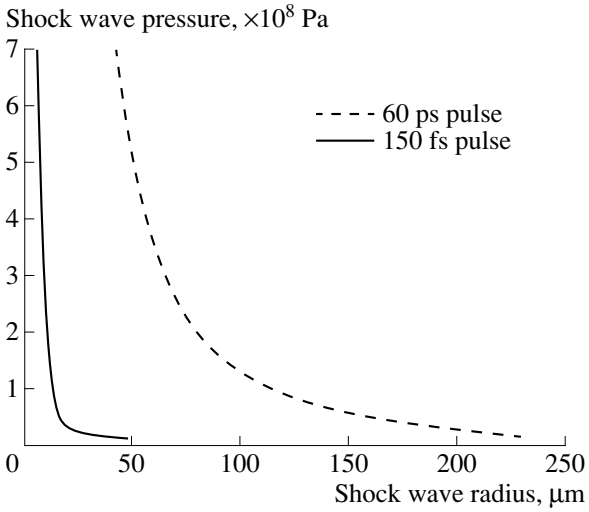

Fig. 2. Shock wave pressure as a function of the shock wave radius in water generated by 150 fs (solid line) and 60 ps (dashed line) laser pulses. Note, that in both cases laser fluences approximately ten times above the threshold were applied.

shown as a function of pulse duration, as measured on the surface of human cornea [8]. While an approximately square root dependence of the fluence threshold on the pulse duration is observed for pulses longer than ~10 ps, below this value the dependence weakens significantly. Recent measurements down to 20 fs pulse durations have again confirmed these observations in corneal tissue [18]. These results suggest an optimal pulse duration for a corneal photodisruptive laser in the few hundred femtosecond pulse duration range, where energy deposited in the tissue is significantly reduced. Further reduction of the laser pulse duration to sub 100-fs level adds significant technical complexity and does not produce any further significant decrease of the threshold [18].

Time-resolved photography of the laser-tissue interaction reveals a marked reduction in shock wave range and cavitation bubble size and their number as the laser pulse duration is decreased to the subpicosecond range [17]. Nonlinear time dependence of the shock wave radius is observed only in the first ~10 ns after femtosecond laser-induced optical breakdown, indicating the rapid decay of the shock wave [17]. Inside the cornea, the dissipation of the shock waves also takes place within approximately 10 ns, corresponding to a radius of about 20 μm.

Similarly, following the analysis of [20], we determined the shock wave pressure generated by femtosecond optical breakdown decay considerably faster than that generated by longer pulses. In Fig. 2, shock wave pressures are shown generated by laser pulses of 60 ps and 150 fs duration. We can estimate the volume of tissue affected by the shock wave if we assume isotropic propagation of the shock wave. We arbitrarily define the range of shock wave as the distance when its pressure decreases below 3×10^7 Pa (at low pressure values, the accuracy of this method is limited [20]). For femtosecond optical breakdown, the shock wave affects a volume of approximately 4×10^{-5} mm^3, while for picosecond pulses the volume is approximately 1000 times higher ($V = 4 \times 10^{-2}$ mm^3). Obviously, even more dramatic reductions are observed if the current results are compared to clinically-available nanosecond photodisruptive lasers, such as the Nd : YAG laser.

Another important secondary effect, creation of a cavitation bubble, occurs with further expansion of the plasma [11–13, 21]. This event is followed by implosion of the cavitation bubbles, which may create secondary acoustic transients, such as radial propagating acoustic waves [21]. The final size of the cavitation bubble determines potential packing strategies for multiple laser spots, and thereby regulates the degree of contiguous effects. A strong reduction in the size of the cavitation bubbles takes place when the duration of the laser pulse is shortened to the 100 fs range when compared to still relatively short picosecond laser pulses [17, 21].

While shock waves and cavitation bubbles may cause extended collateral tissue effects if they reach large magnitudes [22], the primary controlled surgical effect of photodisruptive lasers is most likely due to tissue evaporation by the laser plasma [22]. The consequence of the reduced collateral effects with femtosecond laser pulses is the ability to perform high precision microsurgical procedures without disruption of the corneal surface. With the aid of a high repetition, computer driven high precision beam delivery device, surgeon-dependent factors can also be reduced, thereby increasing standardization.

III. THE FEMTOSECOND MEDICAL LASER

We have designed and built an all-solid-state Nd : glass laser system, able to generate pulses as short as ≈500 fs at a wavelength of 1.06 μm. A schematic of the laser system (Fig. 3) shows the four key components of the system: a laser oscillator, a pulse stretcher, a regenerative amplifier, and a pulse compressor. The Nd : glass oscillator is pumped by a single laser diode and mode-locked by a solid-state saturable absorber, making the pulse formation reliable and self-starting [23]. Intracavity dispersion compensation is provided by Gires-Tournois mirrors, which allow for a compact, folded resonator design. The laser produces a train of 200-fs pulses at a repetition rate of 80 MHz. For chirped pulse amplification, pulses from the output of the oscillator are stretched to a pulse width of approximately 60 ps in a subcompact stretcher unit, which is based on a single holographic transmission grating [24]. Selected pulses are then seeded at a few kHz repetition rate into the regenerative amplifier using a Pockels cell. To achieve required energy ranges, two 2W-diodes are used as pump sources for the Nd : glass gain medium in the amplifier. After maximum amplification, the pulses are dumped out of the amplifier laser at a polarizer by switching the voltage applied to a Pockels cell. The amplified pulses are then re-compressed in a compressor unit, which uses the holographic transmission grating of the stretcher [24]. The duration of the compressed pulses is about 500 fs, which is slightly longer than the oscillator pulse width due to gain narrowing in the amplifier. After compression, the laser pulse energy is measured to be as high as 25 μJ. Losses are primarily due to the non-optimized optics in the compressor. Pulse energies of 50 μJ could be obtained by using higher quality optics in the compressor unit. The pulse repetition rate is adjustable up to as high as 3 kHz, while the spatial intensity profile of the output beam from the Nd : glass laser system was measured to be close to the ideal TEM_{00} mode. We employ a computer-controlled optical scanning system to deliver the amplified femtosecond laser pulses to the tissue. The beam is focused down to a spot diameter of 5 μm within the corneal stroma, using a high numerical aperture focusing objective. A flat contact glass at the end of the delivery system is placed on the surface of the cornea, establishing a reference plane for reproducible intrastromal photodisruption. The position of the eye at the contact glass is fixed by generating a weak vacuum with a suction ring. The current optical system allows a scanning range of within a disc of 9 mm in diameter and 1 mm depth. A surgical microscope with a light source (slit lamp) and video camera is attached to the system for observing the surgical procedure. Scanning of the beam is computer controlled, with real-time monitoring of the laser and delivery system status.

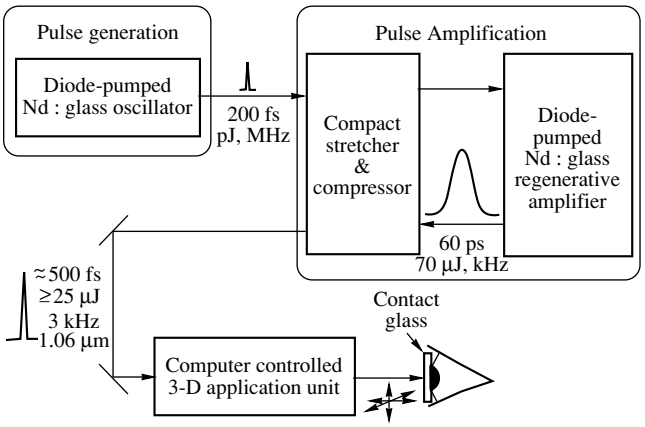

Fig. 3. A schematic of the compact all-solid-state femtosecond laser system and the scanning unit for 3-dimensional movement of the focal spot.

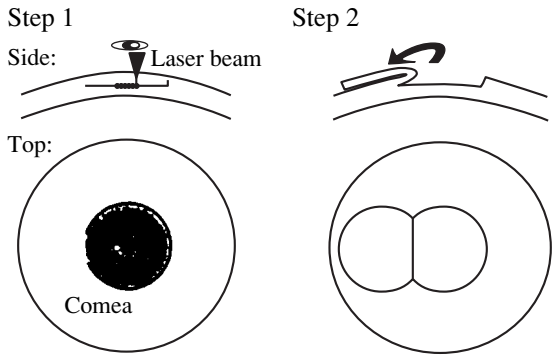

Fig. 4. Schematic of the femtosecond laser flap cutting procedure with side and top views of the treated cornea (see text).

IV. SURGICAL PROCEDURES

A. Corneal Flap Cutting Procedure

Conventionally, a corneal flap is created with a mechanical microkeratome, a motorized blade that gives the excimer laser access to deeper layers of the stroma during laser-assisted in situ keratomileusis (LASIK). For femtosecond laser flap cutting (Fig. 4), the laser focus first is scanned along a spiral pattern inside the corneal stroma at a predetermined depth [25]. The intrastromal cut is followed by several arc-shaped cuts at decreasing depth in the cornea to connect this intrastromal cut to the corneal surface, with a hinge present to maintain connection to the cornea. The contact glass is removed and the flap lifted, similar to what is done in the mechanical procedure.

B. Femtosecond Laser Keratomileusis (FLK)

The goal of this procedure is to perform a LASIK-like procedure with the ultrafast laser, without using an excimer laser to remove tissue from the corneal bed. First, a spiral pattern of the flap procedure is performed

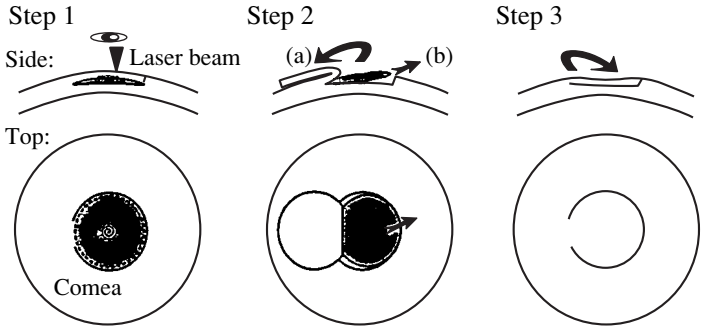

Fig. 5. Schematic overview of the femtosecond laser keratomileusis procedure (see text).

at a predetermined depth, forming the lower surface of a lens (lenticule). After moving the focus closer to the cornea surface, a second curved spiral pattern completes the top surface of the lenticule (Fig. 5). Arc cuts at decreasing depth inside the cornea connect the lenticule to the corneal surface. After removing the contact glass, the lenticule can be exposed and extracted with a forceps. Finally, the flap can be repositioned similar to what is done with a LASIK flap. Due to the missing volume of the lenticule, the surface of the cornea flattens and a change in refractive power is achieved.

C. Femtosecond Laser Intrastromal Vision Correction (FLIVC)

Femtosecond laser intrastromal vision correction was evaluated during preliminary in vivo rabbit and primate studies. For these procedures, layers of spiral patterns were placed at decreasing depths and increasing diameters in the corneal stroma (Fig. 6), resulting in a stack of spirals with increasing diameters. Each spiral layer vaporizes a thin layer of tissue, while several layers yield a significant change in the corneal thickness. Using this approach, appropriate design of stacked layer photodisruption should result in specific refractive changes, without the need of any significant incision.

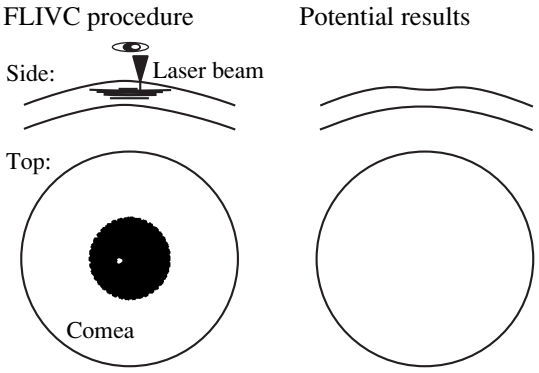

Fig. 6. Schematic of femtosecond laser intrastromal vision correction (see text).

V. ANALYTICALLY SOLVABLE SHELL MODEL OF THE CORNEA

To predict the results of laser refractive corneal surgery, we have developed a shell model for the cornea (see also [26]). The mechanical properties of the thin shells have been analyzed previously in [27]. We show that the predictability of surgical correction given by geometric models [28–31] may be significantly improved using the shell-model under consideration, which takes into account the influence of the intraocular pressure.

The cornea is represented here as an axisymmetric shell with, in general, position-dependent thickness and Young's modulus. The equations describing such a shell were considered earlier in [27] in connection with its mechanical behavior. We use these equations for the radial displacement and the principal curvatures of an axisimmetric shell under the action of a homogeneously distributed hydrostatic pressure to calculate and predict the corrections of the corneal optical power resulting from refractive surgery. The results of various kinds of refractive corneal surgery can be predicted on the basis of the shell-model, by choosing the values and the angle-space distributions for the Young's modulus and the thickness of the cornea corresponding to a given refractive surgical procedure.

In PRK or LASIK-kind refractive surgery, a specific amount of corneal tissue is removed to change corneal curvature. The change in corneal curvature takes place after the collapse of the cavity induced in the cornea after removal of the tissue material. For example, in the case of automated lamellar keratomileusis (ALK) or picosecond laser keratomileusis (PLK) for high myopia described in [28] a block of tissue is removed through a corneal incision from the axial part of the cornea. The myopic correction of vision takes place after the collapse of the intrastromal cavity created by the removal of a corneal lenticule. This collapse is equivalent to removing of an intrastromal lens of the same shape as the cavity.

In most corneal models, the changes in the curvature of the cornea are calculated based on the principles of geometry and geometric optics (geometric models, [28–31]) with no regard to the bio-mechanical response

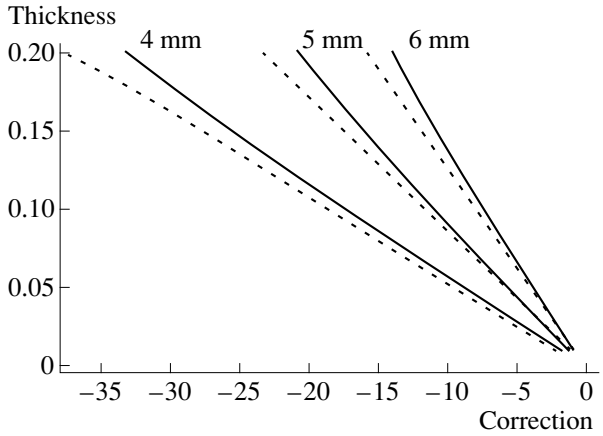

Fig. 7. Dependence of the maximum thickness of the treatment zone to achieve the necessary correction of the refractive power of the cornea for different values of the treatment zone diameter: d_0 = 4, 5, 6 (mm) for Young's modulus E = 10^7 dynes/cw^2 and the maximum thickness of the laser-treated zone h_{00} = 0.2 mm. The solid lines correspond to the shell model, the dotted ones are for the geometric model.

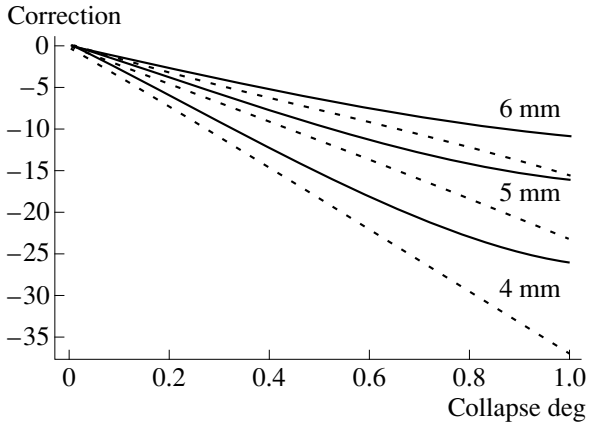

Fig. 8. Dependence of the myopic correction (in Diopters) of corneal optical power on the collapse coefficient κ for different values of the diameter (d_0 = 6, 5, 4 mm) of the treatment zone. Parameters applied: "weakening" parameter β = 0.5, Young's modulus $E = 3 \times 10^7$ dyn/cm^2, the thickness of the treatment zone h_{00} = 0.2 mm, intraocular pressure $P = 2 \times 10^4$ dyn/cm^2. The solid lines are the results based on the shell model, the dotted ones are predictions of the geometric model.

of the cornea, influenced in particular, by the intraocular pressure. Furthermore, a complete collapse of the laser induced cavity is assumed, as a rule, in different corneal models aiming to predict the correction of vision by the refractive corneal surgery. While this is true in the case of PRK, ALK, PLK and LASIK refractive surgery techniques, this assumption fails to be correct in the case of intrastromal corneal photodisruption using femtosecond laser radiation. In the latter case, only a part of the stromal tissue is evaporated, while some of the laser-treated tissue remains with altered mechanical properties.

In contrast to the geometric models, the shell-model allows for description of the bio-mechanical response of the cornea to the action of the laser radiation. The results of the shell-model based calculations of the maximum thickness of the lenticule removed during PLK to obtain a desired optical correction are depicted in Fig. 7 for different values of the diameter of the lentucle, [28]. The predictions of the geometric model are shown by dotted lines in the same figure. While the refractive power corrections predicted by the shell-model are near to those predicted by the geometric model for small myopic corrections, the predictions of the two models differ significantly for larger corrections, as seen in Fig. 7. For a more detailed comparison, the clinical data of myopic correction from [28] are represented in Table 1 with the predictions of the shell-model and those of the geometric model. Good agreement between the predicted and achieved PLK results for myopic correction are seen. Only one fitting parameter, the corneal average Young's modulus was used in calculations utilizing the shell-model.

When intrastromal treatment is performed using femtosecond radiation, only a partial collapse of the laser-treated zone is found with altering of the tissue bio-mechanical properties of this zone. We introduce a coefficient of "weakening" $\beta = E_{tr}/E_{str}$ describing a diminished Young's modulus for

the treated stromal tissue. Here E_{str} is the Young's modulus for the untreated stroma and E_{tr} is the same for the treated one. We describe the degree of the collapse of the laser produced stromal cavity by a coefficient $\kappa = h_0/h_{tr}$, with h_0 being the maximum thickness of the collapsed part of the stromal laser-treated part and h_{tr} being the maximum thickness of the all laser-treated zone of the stroma. The value of the parameter κ is between zero and unity. Zero of κ corresponds to no evaporation (no collapse) of the treated part of the stroma, while the value equal to unity corresponds to the complete evaporation and removal of the stromal tissue, accompanied by the complete collapse of the laser-induced cavity. The dependence of the myopic corneal correction on the collapse coefficient κ is shown in Fig. 8. The treatment zone is assumed to have an ellipsoid form of the in the numerical simulations.

Picosecond laser keratomileusis: Comparison of predictions for myopic corrections Δk (in Diopters) of the shell and geometric models with the clinical data of [28] (see text). The effective averaged corneal Young's modulus is $E = 0.45 \times 10^7$ dyn/cm^2

The size diameter/thickness	Δk(D), [8] (clinical results)	Δk(D), shell-model	Δk(D), geometric model
4 mm/100 μm	–11.3(±0)	–11.7	–18.1
4 mm/120 μm	–13.1(±2.7)	–13.2	–21.88
3.2 mm/120 μm	–19.6(±2.3)	–21.68	–34.75

VI. CONCLUSION

The highly-localized tissue effects associated with femtosecond laser photodisruption led us to construct a practical femtosecond laser system for clinical testing. Subsequent studies have demonstrated effective in vitro and in vivo corneal photodisruption performing novel femtosecond procedures (corneal flap cutting, laser keratomileusis and intrastromal vision correction). While these studies require validation in humans, femtosecond laser devices show promise in high-precision, minimally-invasive surgical applications. As femtosecond tools and procedures develop in the coming years, significant advantages over current mechanical and laser devices and techniques will be required to gain clinical acceptance.

An analytically solvable shell-model of the cornea has been developed to predict the results of the refractive corneal procedures. Comparison of calculations based on the shell-model with clinically obtained results suggest a promising approach using this model. The ability of the shell-model to describe the biomechanical response of the cornea to entirely intrastromal photodisruption by femtosecond laser pulses may make the shell-model a valuable tool in developing effective surgical strategies.

REFERENCES

1. Boulnois, J.-L., 1986, *Lasers in Medical Science*, **1**, 47.
2. Niemz, M.H., 1996, *Laser Tissue Interactions: Fundamentals and Applications* (Heidelberg: Springer).
3. Puliafito, C.A. and Steinert, R.F., 1984, *IEEE J. Quantum Electron.*, **20**, 1442.
4. Stern, D., Schoenlein, R.W., Puliafito, *et al.*, 1989, *Arch. Ophthalmol.*, **107**, 587.
5. Niemz, M.H., Hoppeler, T., Juhasz, T., and Bille, J.F., 1993, *Lasers and Light in Ophthalmol.*, **5**, 149.
6. Bloembergen, N., 1974, *IEEE J. Quantum Electron.*, **10**, 375.
7. Docchio, F., Sacchi, C.A., and Marshall, J., 1986, *Lasers Ophthalmol.*, **1**, 83.
8. Loesel, F.H., Niemz, M.H., Bille, J.F., and Juhasz, T., 1996, *IEEE J. Quantum Electron.*, **32**, 1717.
9. Kennedy, P.K., Boppart, S.A., Hammer, D.X., *et al.*, 1995, *IEEE J. Quantum Electron.*, **31**, 2241.
10. Bell, C.E. and Landt, J.A., 1967, *Appl. Phys. Lett.*, **10**, 46.
11. Zysset, B., Fujimoto J.G., and Deutsch, T.F., 1989, *Appl. Phys. B*, **48**, 139.
12. Fujimoto, J.G., Lin, W.Z., Ippen, E.P., *et al.*, 1985, *Invest. Ophthalmol. Vis. Sci.*, **26**, 1771.
13. Vogel, A., Hentschel, W., Holzfuss, J., and Lauterbom, W., 1986, *Ophthalmol.*, **93**, 1259.
14. Kurtz, R.M., Liu, X., Elner, V.M., *et al.*, 1997, *J. of Refractive Surgery*, **13**, 653.
15. Kautek, W., Mitterer, S., Krüger, J., *et al.*, 1994, *Appl. Phys. A*, **58**, 513.
16. Hammer, D.X., Thomas, R.J., Noojin, G.D., *et al.*, 1996, *IEEE J. Quant. Electron.*, **32**, 670.
17. Juhasz, T., Kastis, G.A., Suarez, C., *et al.*, 1996, *Lasers Surg. Med.*, **19**, 23.
18. Loesel, F.H., Tien, A.-C., Backus, S., *et al.*, 1999, *Proc. SPIE*, **3565**, in press.
19. Squier, Du, J., Kurtz, R.M., Elner, V., *et al.*, 1995, in *Ultrafast Phenomena IX*, Barbara, P.F. *et al.*, Ed. (New York: Springer), 254.
20. Doukas, A.G., Zweig, A.D., Frisoli, J.K., *et al.*, 1991, *Appl. Phys. B*, **53**, 237.
21. Juhasz, T., Hu, X.H., Turi, L., and Bor, Z., 1994, *Lasers Surg. Med.*, **15**, 91.
22. Vogel, A., Schweiger, P., Freiser, A., *et al.*, 1990, *IEEE J. Quant. Electron.*, **26**, 2240.
23. Keller, U., Weingarten, K.J., Kärtner, F.X., *et al.*, 1996, *IEEE J. Select. Topic Quant. Electron.*, **2**, 435.
24. Horvath, C., Braun, A., Liu, H., *et al.*, 1997, *Opt. Lett.*, **22**, 1790.
25. Kurtz, R., Horvath, C., Liu, H., *et al*., 1998, *J. Refractive Surgery*, **14**, 541.
26. Rand, R.H., Lubkin, S.R., Howland, H.C., 1991, *J. Biomech. Engin.*, **113**, 239.
27. Timoshenko, S. and Woinowsky-Krieger, S., 1959, *Theory of Plates and Shells* (N.Y.: McGraw-Hill).
28. Bryant, M.R. and Juhasz, T., 1999, *J. Refractive Surgery* (submitted).
29. Munnerlyn, C.R., Koons, S.J., and Marshall, J., 1988, *J. Cataract. Refract. Surg.*, **14**, 46.
30. Blaker, W.J. and Hersh, P.S., 1994, *J. Refractive Surgery*, **10**, 125.
31. Colliac, J.P., Shammas, J.H., and Bart, D.J., 1994, *Am. J. Ophthalmol.*, **117**, 369.